Chemical and biological sensors

# Flexible Electrochemical Sensor for Interleukin-6: Toward Wearable Cytokine Monitoring

Moritz Ploner[1], Bajramshahe Shkodra[1], Antonio Altana[1,2], Mattia Petrelli[1], Anna Tagliaferri[1], Daniele Resnati[3], Paolo Lugli[1,2*], Martina Aurora Costa Angeli[1], and Luisa Petti[1**]

[1] *Sensing Technologies Laboratory (STL), Faculty of Engineering, Free University of Bozen-Bolzano, 39100 Bozen, Italy*
[2] *Competence Centre for Mountain Innovation Ecosystems, Free University of Bozen-Bolzano, 39100 Bozen, Italy*
[3] *Empatica Srl, 20144 Milano, Italy*
[*] *Fellow, IEEE*
[**] *Senior Member, IEEE*

Manuscript received 31 May 2024; revised 21 June 2024; accepted 4 July 2024. Date of publication 17 July 2024; date of current version 26 July 2024.

Abstract—The detection of cytokines, which are key proteins involved in immune system signaling, is of extreme importance for health monitoring. Among the various cytokines, interleukin-6 (IL-6) is particularly interesting to monitor, also considering that sweat IL-6 levels show a significant correlation with blood levels, in the range of pg/mL. Despite its importance, sensitive and wearable detection of IL-6 in sweat is still lagging behind. In this work, we fabricated and characterized a flexible screen-printed carbon-based three-electrode electrochemical sensor for IL-6 detection. The planar electrochemical sensor was first modified with gold nanoparticles (AuNPs) and then biofunctionalized with thiolated aptamers. The characterization via electrochemical impedance spectroscopy (EIS) demonstrated selective IL-6 detection in the range from 0.2 to 20 pg/mL in artificial sweat, perfectly covering the physiological range of interest. Our results suggest the potential integration of the developed flexible sensor into wearable devices for cytokine monitoring.

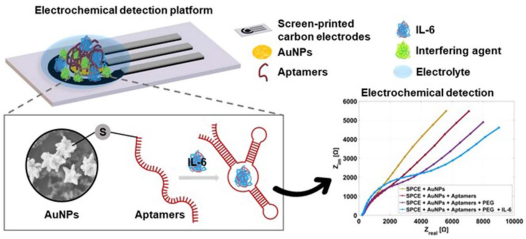


Index Terms—Chemical and biological sensors, aptamer, electrochemical sensor, cytokines, interleukin-6 (IL-6), screen-printed, gold nanoparticles (AuNPs), wearable, sweat.

## I. INTRODUCTION

Standard biomarker monitoring relies on invasive blood tests and time-consuming lab analysis. Alternatively, wearable sensors enable continuous and minimally invasive monitoring of multiple human health indicators in biofluids externally accessible, such as sweat [1]. Sweat contains a wealth of physiological information, including cytokines, which are compelling biomarkers for human health monitoring as their detection offers insights into several physiological and pathological processes [2]. Among the various cytokines, the immune response regulator interleukin-6 (IL-6) is the most common electrochemically detected cytokine in sweat [3], as its detection enables insight into various pathologies, such as cancer and sepsis [3]. Moreover, sweat IL-6 levels show a significant correlation with blood levels [4], enabling its noninvasive monitoring via wearable devices [5]. A widely employed electrochemical platform for the detection of IL-6 is the three-electrode system, consisting of a working electrode (WE), a counter electrode (CE), and a reference electrode (RE) [3]. This system can be fabricated cost-effectively and on flexible substrates, e.g., utilizing screen printing methods [6], allowing its integration into wearable applications. For sensitive cytokine detection, the three-electrode platform is often paired with electrochemical impedance spectroscopy (EIS) and cyclic voltammetry (CV) [7], essential electroanalytical methods that provide high sensitivity crucial for accurate biological analysis [8].

Considering the low physiological levels of IL-6 in sweat, ranging from 5 to 15 pg/mL [7], highly sensitive detection techniques are required [3]. For instance, this could be done by using nanomaterials, such as gold nanoparticles (AuNPs), which are able to increase the electron transfer and biofunctionalization, and are bio-compatible [9]. In fact, AuNPs can be easily immobilized onto screen-printed carbon electrode (SPCE) surfaces using an electrochemical deposition technique with control over size, shape, and density by adjusting the deposition parameters, such as applied potential and deposition time [10]. This work presents the fabrication, optimization, and characterization of a flexible and selective SPCE system, with a WE twofold smaller than the commercially available platforms, to detect IL-6. AuNPs were electrodeposited on the WE, and subsequently biofunctionalized with IL-6 thiolated aptamers. The IL-6 AuNP-aptamer-modified sensor enabled detection of IL-6 in the linear range from 0.2 to 20 pg/mL in artificial sweat. Furthermore, the sensor demonstrated selectivity *vs.* the interfering agent tumor necrosis factor-alpha (TNF-$\alpha$), showing negligible responses.

## II. MATERIALS AND METHODS

All unspecified chemicals were purchased from Sigma-Aldrich.

Corresponding author: Moritz Ploner (e-mail: moritz.ploner@student.unibz.it).
Associate Editor: Hamida Hallil.
Digital Object Identifier 10.1109/LSENS.2024.3429627

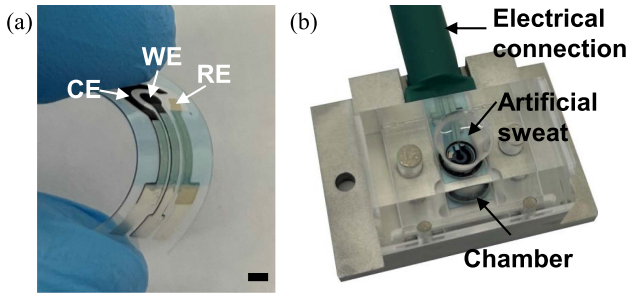


Fig. 1. In-house screen-printed and flexible three-electrode sensor. (a) Image showing working, counter, and RE (WE, CE, and RE, respectively, with a scale bar of 3 mm). (b) Image of experimental setup utilized for the measurement of its response.

### A. Transducer Fabrication

The fully screen-printed sensor layout consists of WE (with a diameter of 2 mm, twofold smaller than the commercially available Metrohm DropSens) and CE, both made of carbon (LOCTITE EDAG PF 407 C) and a silver/silver chloride (LOCTITE EDAG PE 409 E&C) RE. To ensure the flexibility of the sensors for skin conformity, the device was fabricated on a polyethylene terephthalate (PET) substrate, as shown in Fig. 1(a). To reduce the sheet resistance of the platform, the connection parts of the three electrodes were coated by screen-printing a second layer of a conductive silver paste (LOCTITE ECI 1010 E&C). After each printing step, the printed layer was cured at 120 °C for 15 min. Finally, a dielectric layer (Applied Ink Solutions PE-TD-642) was first screen-printed, to passivate the tracks and allow exposure only to the active area, and then cured at 130 °C for 5 min. All the inks and PET for the screen-printing process were purchased from LOCTITE E&C (CA, USA).

### B. AuNP Deposition

Prior to any modifications, the SPCEs underwent CV electrochemical cleaning in 0.1 M potassium chloride (KCl), scanning from −2 to 2 V at a scan rate of 100 mV/s for 20 cycles, to improve electron transfer kinetics and reduce device-to-device variability by removing surface impurities [11]. All electrochemical procedures were conducted using a potentiostat (VersaSTAT 4, Princeton Applied Research, USA).

AuNP electrodeposition on the WE was performed using a solution containing 0.5 mM chloroauric acid in 0.5 M sulfuric acid employing chronoamperometry. The reduction potential of AuNPs of 0.54 V was extracted from the CV, conducted in the deposition solution (scanning from −1 to 1 V at a scan rate of 100 mV/s) and set as the potential for the chronoamperometric deposition. AuNPs were deposited for different times, specifically 50, 100, 200, 400, 600, and 1000 s. Subsequently, the active area of the AuNP-modified WE at different deposition times was calculated by performing CV in 5 mM of ferricyanide/ferrocyanide ($Fe[(CN)_6]^{3-/4-}$) in 0.1 M KCl at a scan rate of 100 mV/s.

The morphological properties of the AuNP-modified WE were characterized using a scanning electron microscope (SEM) (JSM-IT 100, JEOL, Japan) operating at a voltage of 3 V, a working distance of 8 mm, magnification of 10.00 K X and an aperture size of 20 μm.

### C. Aptamer Biofunctionalization

IL-6 aptamers thiolated at the 3' end were purchased from Microsynth AG, Switzerland, with the following sequence: 5'-GGTGGCAGGAGGACTATTTATTTGCTTTTCT-3' [12].

Before functionalization, the aptamers were treated with 50-fold tris(2-carboxyethyl) phosphine (TCEP) excess relative to IL-6 aptamer concentration (100 μM) for 1 h, to reduce the disulfide bonds. Next, the aptamer solution was diluted in 1x phosphate-buffered saline (PBS) to a concentration of 5 μM, and cleaned with Zeba spin desalting columns [13].

Before functionalization, the aptamers were denatured at 95 °C for 5 min and then renatured by cooling down to room temperature [14]. Subsequently, 10 μL of 5 μM aptamer solution was drop-casted on the AuNP-modified WE and incubated for 24 h at 4 °C and 100% humidity [15]. Next, the functionalized sensors were incubated for two hours in 10 μL of 500 μM poly(ethylene glycol) (PEG), to prevent nonspecific interactions [16]. To confirm successful biofunctionalization, first EIS was performed in 70 μL of 2 mM of ferricyanide ($Fe[(CN)_6]^{3-}$) in 1x PBS [13] in a frequency range from 0.1 to 100 kHz, with $V_{DC}$ set to 0.11 V and $V_{AC}$ set to 10 mV, for all the functionalization steps. To further confirm successful biofunctionalization, CV was performed in 70 μL of 2 mM of ferricyanide ($Fe[(CN)_6]^{3-}$) in 1x PBS within a potential range from −0.4 to +0.6 V at a scan rate of 100 mV/s for all the functionalization steps.

### D. Biosensor Characterization

To validate the biosensor behavior, different concentrations of IL-6, i.e., 0.2, 0.5, 2, 5, 10, 20, and 200 pg/mL, were prepared in 1x PBS and artificial sweat. Artificial sweat was prepared in deionized water, containing 8 mM KCl, 30 mM sodium chloride, 0.084 mM creatinine, 0.17 mM glucose, 0.059 mM uric acid and 0.01 mM ascorbic acid [17]. First, EIS was performed for all concentrations in 1x PBS on two different sets of samples ($N = 7$) in a frequency range from 0.1 Hz to 100 kHz. $V_{DC}$ was set to 0.11 V, and $V_{AC}$ was set to 10 mV.

Initially, an EIS measurement was carried out in 50 μL 1x PBS, which served as a baseline. Subsequently, increasing concentrations of IL-6 were added to the chamber, and the EIS response was recorded.

The impedance magnitude was derived from the EIS response at 10 Hz for the different IL-6 concentrations. Subsequently, for each concentration, the impedance magnitude was normalized by subtracting the baseline impedance value measured in 1x PBS. Second, CV was performed in all concentrations in 1x PBS on two different sets of samples ($N = 7$) within a potential range from −0.4 to +0.6 V at a scan rate of 100 mV/s.

Given the higher sensitivity of EIS compared to CV, EIS was employed for detecting IL-6 in artificial sweat, in the same manner described above. The validation in 1x PBS and artificial sweat was performed using the setup shown in Fig. 1(b).

## III. RESULTS AND DISCUSSION

### A. AuNP Deposition

To determine the ideal deposition time, the active area of the WE was extrapolated for different deposition times ($N = 3$). The Randles–Sevcik model, in combination with $[Fe(CN)_6]^{3-/4-}$ as a redox system, was utilized given its suitability for single electron transfer [18]. With longer deposition time, the density of AuNPs increased, leading to a higher surface area, peaking at 600 s.

At a deposition time of 1000 s, the effect saturated due to the formation of a continuum gold film rather than nanoparticles, resulting in reduced roughness and thus active area [19]. The highest active area, corresponding at 0.0039 $cm^2$, was achieved for a deposition time of 600 s, representing a 131% increase compared to the calculated area of the bare electrode (0.0017 $cm^2$), and indicating more binding sites available for the biofunctionalization.

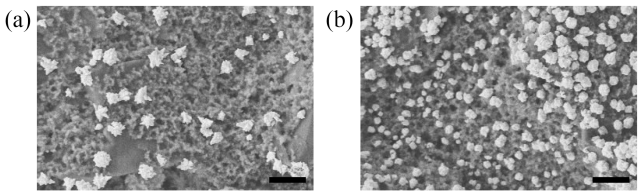


Fig. 2. AuNP deposition. (a) SEM image of WE for a deposition time of 100 s. (b) 400 s, with scale bar of 1 μm.

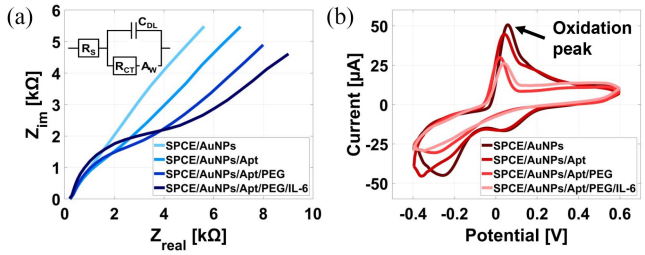


Fig. 3. (a) EIS showing changes in the charge transfer resistance $R_{CT}$. (b) CV demonstrating changes in the oxidation peak current with increasing modification complexity. More complex modification impedes the ferricyanide molecule from accessing the electrode surface. (Apt: Aptamer.)

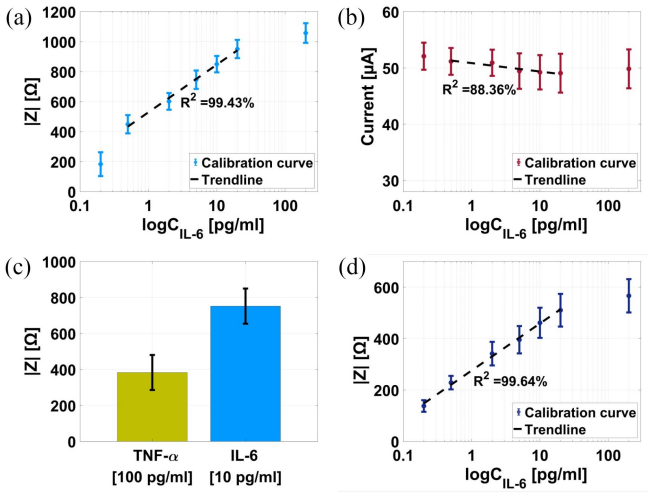


Fig. 4. (a) Calibration curve, magnitude of impedance for different concentrations of IL-6 in 1x PBS. (b) Calibration curve, oxidation peak current during CV for different concentrations of IL-6 in 1x PBS. (c) The biosensor responded minimally to TNF-$\alpha$, even at concentrations ten times higher than those of the IL-6 target. (d) Calibration curve, magnitude of impedance for different concentrations of IL-6 in artificial sweat. Error bars represent the standard deviation with $N = 7$ per concentration.

## B. Aptamer Biofunctionalization

Each step of the WE functionalization was tracked by evaluating the change of the Nyquist plots of the EIS response, in particular the charge transfer resistance ($R_{CT}$, i.e., the semicircle diameter), and by evaluating the change of the oxidation peak current during CV.

Fig. 3(a) shows the Nyquist plot of the EIS data, fitted to a Randles circuit. The bare AuNP-modified SPCE displayed a linear behavior with a negligible small semicircle representing the $R_{CT}$ ($1.6 \pm 0.4\ \Omega$) of electrochemical reactions at high frequencies. Upon biofunctionalization with aptamers, the semicircle of the Nyquist plot increased due to hindered diffusion of $Fe[(CN)_6]^{3-}$ to the electrode surface by the aptamer layer ($196 \pm 58.5\ \Omega$). Subsequent PEG coating further improved the charge transfer resistance $R_{CT}$ ($648.7 \pm 249.1\ \Omega$), confirming the formation of a blocking layer on the surface of the electrode [15]. Following incubation with IL-6, the radius of the semicircle was enhanced further, indicating the binding of the IL-6 target by the aptamer. This increase in $R_{CT}$ ($1780 \pm 282.8\ \Omega$), upon the binding event, suggested aptamer backbone rearrangement, which impeded the diffusion of $Fe[(CN)_6]^{3-}$ to the electrode surface [12]. Successful functionalization is once more underlined when comparing the cyclic voltammograms displayed in Fig. 3(b). For the bare AuNP-modified SPCE the highest oxidation peak current is achieved ($58.28 \pm 7.74\ \mu A$). For subsequent biofunctionalization with aptamers, the current decreased ($51.12 \pm 13.39\ \mu A$), as the diffusion of $Fe[(CN)_6]^{3-}$ to the electrode surface by the aptamer layer is hindered. The current further decreases after PEG coating ($40.29 \pm 2.13\ \mu A$), which confirmed the formation of a blocking layer. Upon incubation with IL-6, the oxidation peak current further decreased, suggesting aptamer backbone rearrangement to impede further $Fe[(CN)_6]^{3-}$ diffusion ($29.85 \pm 1.98\ \mu A$) [15].

## C. Biosensor Response

To evaluate the response of the sensor toward different concentrations of IL-6 in 1x PBS (pH of 7.4), the magnitude of the impedance was extracted at a frequency of 10 Hz, as depicted in Fig. 4(a). As the concentration of IL-6 increased, the magnitude of the impedance improved, as expected. At higher concentrations of IL-6, more binding events with the aptamer occurred. The binding event causes the aptamer to undergo a conformational change, resulting in bending. This movement brings the negatively charged backbone of the IL-6 aptamers closer to the sensor surface, resulting in an increase in negative charge density and consequently, an increase in the absolute value of impedance [20].

For the CV response, the peak current for different concentrations of IL-6 in 1x PBS was extracted, as displayed in Fig. 4(b). The peak current decreased with higher concentrations of IL-6 since more binding events with the aptamer occurred. Comparing both EIS and CV as detection methods, the higher sensitivity of EIS [317.57 Ω/log(pg/ml)] in comparison to the sensitivity of the CV response [−1.5 μA/log(pg/ml)] is evident, as also confirmed in [9]. Moreover, the EIS response showed a higher linearity ($R^2 = 99.43\%$) compared to the CV response ($R^2 = 88.36\%$).

At a concentration of 200 pg/mL, the sensor's binding capacity saturated, resulting in a plateau in the observed signal for EIS and CV response. Similar behavior was also observed by Kumar et al. [9], who developed an AuNP-aptamer-modified gold electrode and employed EIS as a detection method, with the sensor saturating at a concentration of 20 pg/mL.

Fig. 4(c) depicts the study of the cross-selectivity. The green column shows the sensor response in the presence of 100 pg/mL of TNF-$\alpha$ interfering agent in 1x PBS, while the blue column shows the response when adding 10 pg/mL IL-6 to the 100 pg/mL of TNF-$\alpha$ in 1x PBS. Remarkably, despite the TNF-$\alpha$ concentration being ten times higher than that of the target analyte (IL-6), the sensor showed insensitivity to TNF-$\alpha$, as evidenced by the negligible change in impedance magnitude. Indeed, upon introducing the IL-6 an immediate increase in impedance was observed independent of the interfering agent present in the solution, highlighting the high selectivity and sensitivity of our AuNP-modified SPCE aptasensors.

Due to its higher sensitivity compared to CV, EIS was employed for detecting IL-6 in artificial sweat. The EIS response in artificial sweat (pH of 5.4), depicted in Fig. 4(d), showed good sensitivity [183.26 Ω/log(pg/ml)] and a high coefficient of determination of 99.63% in the range from 0.2 to 20 pg/mL, effectively covering the physiological range of IL-6 in human sweat. In comparison,

Table 1. State-of-the-art Three-Electrode AuNP-Modified Aptasensors for the Electrochemical Detection of IL-6 in Sweat

| Substrate | Redox reporter | Linear range [pg/mL] | LOD [pg/mL] | Ref. |
|---|---|---|---|---|
| Rigid | $Fe[(CN)_6]^{3-/4-}$ | 0.02–20 | 0.02 | [9] |
| Flexible | / | 0.2–20 | 0.2 | This work |

the sensitivity in the range of interest in 1x PBS was calculated as 317.57 Ω/log(pg/ml), with a linearity of 99.43%. The higher sensitivity of the sensor in 1x PBS was expected as the artificial sweat represents a more complex medium than the buffer.

Different aptamer-based IL-6 biosensors were presented in the past by other researchers [12], [15], [21], however focusing on the detection of IL-6 in biofluids besides sweat, or employing transducers other than three-electrode platforms. To the best of the authors' knowledge, only Kumar et al. [9] published on the aptameric detection of IL-6 in sweat using a three-electrode platform. Our sensor achieves a limit of detection (LOD) of 0.2 pg/mL, and shows comparable performance with the sensor presented by Kumar et al. [9] (see Table 1). In the platform of Kumar et al. [9], gold was used as WE (modified with AuNPs) and platinum as CE, resulting in a lower LOD (LOD of 0.02 pg/mL), but also higher cost compared to our carbon-based screen-printed platform. In addition, the detection method of Kumar et al. [9] relied on redox reporters supporting the detection, making the method more complex and unsuitable for wearables. Instead, the sensor presented in this work employed AuNPs on SPCE as nanomaterials, emphasizing simplicity and cost-effectiveness, as well as novelty employing EIS as a detection method allowing to avoid the use of redox reporters. Furthermore, unlike the sensor discussed above, our biosensor is designed with flexibility and reduced dimensions in view of wearable applications.

## IV. CONCLUSION

In this letter, we successfully fabricated and characterized an electrochemical biosensor for IL-6 detection in sweat. The AuNP-aptamer-modified biosensor was able to detect IL-6 in its physiological sweat range from 5 to 15 pg/mL. Importantly, the sensor exhibited negligible response to nonspecific analytes, even at a concentration ten times higher than that of IL-6.

The planar and flexible structure of the sensor, coupled with a good sensitivity (LOD of 0.2 pg/mL), makes it well-suited for integration into wearable devices for sweat-sensing applications. Future studies will focus on assessing the sensor's performance under constant sweat flow using microfluidic techniques to simulate real-life scenarios. Moreover, this approach holds promise for expanding the sensor's capabilities to detect a broader range of cytokines, each requiring its own calibration curve. Integration into a sensor array for simultaneous detection of multiple cytokines could significantly enhance understanding of pathological processes, potentially leading to improved disease diagnosis and monitoring.

## ACKNOWLEDGMENT

The work was partially supported by the European Union Next-GenerationEU (PIANO NAZIONALE DI RIPRESA E RESILIENZA (PNRR) - MISSIONE 4 COMPONENTE 2, INVESTIMENTO 3.3 - Decreto del Ministero dell'Università e della Ricerca n.352 del 09/04/2022) within the Advanced-Systems Engineering Ph.D. Program at the Free University of Bozen/Bolzano and is conducted in cooperation with the company Empatica, which is co-financing the project. This work is partially funded by the ON Foods project (project code PE00000003).

The authors would like to thank EMERGE project, European Union's Horizon 2020 research and innovation program, grant agreement number 101008701, and the FH Johanneum, Graz, Austria, for their help in providing instrumentation for SEM measurements.

## REFERENCES

[1] J. Kim, A. S. Campbell, B. E.-F. de Ávila, and J. Wang, "Wearable biosensors for healthcare monitoring," *Nature Biotechnol.*, vol. 37, no. 4, pp. 389–406, 2019.

[2] C. Liu, D. Chu, K. Kalantar-Zadeh, J. George, H. A. Young, and G. Liu, "Cytokines: From clinical significance to quantification," *Adv. Sci.*, vol. 8, no. 15, 2021, Art. no. 2004433.

[3] M. Ploner et al., "A comprehensive review on electrochemical cytokine detection in sweat," *Cell Rep. Phys. Sci.*, 2024.

[4] A. Marques-Deak et al., "Measurement of cytokines in sweat patches and plasma in healthy women: Validation in a controlled study," *J. Immunological Methods*, vol. 315, no. 1–2, pp. 99–109, 2006.

[5] L. E. McCrae, W.-T. Ting, and M. M. Howlader, "Advancing electrochemical biosensors for interleukin-6 detection," *Biosensors Bioelectronics: X*, vol. 13, 2023, Art. no. 100288.

[6] N.-B. Mincu, V. Lazar, D. Stan, C. M. Mihailescu, R. Iosub, and A. L. Mateescu, "Screen-printed electrodes (SPE) for in vitro diagnostic purpose," *Diagnostics*, vol. 10, no. 8, 2020, Art. no. 517.

[7] N. Dutta, P. B. Lillehoj, P. Estrela, and G. Dutta, "Electrochemical biosensors for cytokine profiling: Recent advancements and possibilities in the near future," *Biosensors*, vol. 11, no. 3, 2021, Art. no. 94.

[8] H. Beitollahi, S. Tajik, H. Parvan, H. Soltani, A. Akbari, and M. H. Asadi, "Nanostructured based electrochemical sensor for voltammetric determination of ascorbic acid in pharmaceutical and biological samples," *Anal. Bioanal. Electrochem.*, vol. 6, no. 1, pp. 54–66, 2014.

[9] L. S. Kumar, X. Wang, J. Hagen, R. Naik, I. Papautsky, and J. Heikenfeld, "Label free nano-aptasensor for interleukin-6 in protein-dilute bio fluids such as sweat," *Anal. Methods*, vol. 8, no. 17, pp. 3440–3444, 2016.

[10] I. Anshori et al., "Gold nanospikes formation on screen-printed carbon electrode through electrodeposition method for non-enzymatic electrochemical sensor," *Metals*, vol. 12, no. 12, 2022, Art. no. 2116.

[11] M. A. Alonso-Lomillo, O. Domínguez-Renedo, L. Ferreira-Gonçalves, and M. J. Arcos-Martínez, "Sensitive enzyme-biosensor based on screen-printed electrodes for ochratoxin a," *Biosensors Bioelectron.*, vol. 25, no. 6, pp. 1333–1337, 2010.

[12] M. Tertiş, B. Ciui, M. Suciu, R. Săndulescu, and C. Cristea, "Label-free electrochemical aptasensor based on gold and polypyrrole nanoparticles for interleukin 6 detection," *Electrochimica Acta*, vol. 258, pp. 1208–1218, 2017.

[13] N. Nakatsuka, A. Faillétaz, D. Eggemann, C. Forró, J. Voros, and D. Momotenko, "Aptamer conformational change enables serotonin biosensing with nanopipettes," *Anal. Chem.*, vol. 93, no. 8, pp. 4033–4041, 2021.

[14] B. Shkodra et al., "Polymeric integration of structure-switching aptamers on transistors for histamine sensing," *Faraday Discuss.*, vol. 250, pp. 43–59, 2024.

[15] Y. Li, X. Hua, J. Wang, and B. Jin, "cMWCNT/CoHCF/AuNPs nanocomposites aptasensor for electrochemical detection of interleukin-6," *Talanta Open*, vol. 7, 2023, Art. no. 100188.

[16] Y. Horiguchi, S. Miyachi, and Y. Nagasaki, "High-performance surface acoustic wave immunosensing system on a PEG/aptamer hybridized surface," *Langmuir*, vol. 29, no. 24, pp. 7369–7376, 2013.

[17] M. Petrelli et al., "Method for instability compensation and detection of ammonium in sweat via conformal electrolyte-gated field-effect transistors," *Org. Electron.*, vol. 122, 2023, Art. no. 106889.

[18] B. Shkodra et al., "A PEDOT: PSS/SWCNT-coated screen printed immunosensor for histamine detection in food samples," in *Proc. 2020 IEEE Int. Symp. Circuits Syst. (ISCAS)*, 2020, pp. 1–4.

[19] M. N. Karim and H. J. Lee, "Amperometric phenol biosensor based on covalent immobilization of tyrosinase on au nanoparticle modified screen printed carbon electrodes," *Talanta*, vol. 116, pp. 991–996, 2013.

[20] A. Baraket et al., "A fully integrated electrochemical biomems fabrication process for cytokine detection: Application for heart failure," *Procedia Eng.*, vol. 87, pp. 377–379, 2014.

[21] M. Tertis, P. I. Leva, D. Bogdan, M. Suciu, F. Graur, and C. Cristea, "Impedimetric aptasensor for the label-free and selective detection of interleukin-6 for colorectal cancer screening," *Biosensors Bioelectron.*, vol. 137, pp. 123–132, 2019.

Open Access funding provided by 'Libera Università di Bolzano' within the CRUI CARE Agreement